AD/A-007 043

STUDY OF TWO AUTOMATIC SHORT-PERIOD SIGNAL DETECTORS. TECHNICAL REPORT NUMBER 9. VELA NETWORK EVALUATION AND AUTOMATIC PROCESSING RESEARCH

Stephen S. Lane

Texas Instruments, Incorporated

Prepared for:

Air Force Technical Applications Center
Advanced Research Projects Agency

6 December 1974

DISTRIBUTED BY:

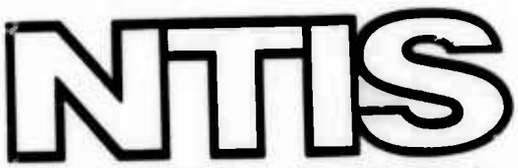

National Technical Information Service
U. S. DEPARTMENT OF COMMERCE

ALEX(01)-TR-74-09

ARPA-0170-43

STUDY OF TWO AUTOMATIC SHORT-PERIOD SIGNAL DETECTORS

TECHNICAL REPORT NO. 9

VELA NETWORK EVALUATION AND AUTOMATIC PROCESSING RESEARCH

Prepared by
Stephen S. Lane

TEXAS INSTRUMENTS INCORPORATED
Equipment Group
Post Office Box 6015
Dallas, Texas 75222

Prepared for

AIR FORCE TECHNICAL APPLICATIONS CENTER
AFTAC Project No. VELA T/4705/B/ETR
Alexandria, Virginia 22314

Sponsored by

ADVANCED RESEARCH PROJECTS AGENCY
Nuclear Monitoring Research Office
ARPA Program Code No. 4F10
ARPA Order No. 2551

6 December 1974

Acknowledgment: This research was supported by the Advanced Research Projects Agency, Nuclear Monitoring Research Office, under Project VELA-UNIFORM, and accomplished under the technical direction of the Air Force Technical Applications Center under Contract No. F03606-74-C-0033.

Reproduced by
NATIONAL TECHNICAL
INFORMATION SERVICE
U S Department of Commerce
Springfield VA 22151

UNCLASSIFIED

SECURITY CLASSIFICATION OF THIS PAGE (When Data Entered)

REPORT DOCUMENTATION PAGE		READ INSTRUCTIONS BEFORE COMPLETING FORM
1 REPORT NUMBER	2 GOVT ACCESSION NO.	3 RECIPIENT'S CATALOG NUMBER
4 TITLE (and Subtitle) STUDY OF TWO AUTOMATIC SHORT-PERIOD SIGNAL DETECTORS		5 TYPE OF REPORT & PERIOD COVERED Technical
		6 PERFORMING ORG REPORT NUMBER ALEX(01)-TR-74-09
7 AUTHOR(s) Stephen S. Lane		8 CONTRACT OR GRANT NUMBER(s) F08606-74-C-0033
9 PERFORMING ORGANIZATION NAME AND ADDRESS Texas Instruments Incorporated Equipment Group Dallas, Texas 75222		10 PROGRAM ELEMENT, PROJECT, TASK AREA & WORK UNIT NUMBERS VELA T/4705/B/ETR
11 CONTROLLING OFFICE NAME AND ADDRESS Advanced Research Projects Agency Nuclear Monitoring Research Office Arlington, Virginia 22209		12 REPORT DATE 6 December 1974
		13 NUMBER OF PAGES 32
14 MONITORING AGENCY NAME & ADDRESS (if different from Controlling Office) Air Force Technical Applications Center VELA Seismological Center Alexandria, Virginia 22314		15 SECURITY CLASS. (of this report) UNCLASSIFIED
		15a DECLASSIFICATION/DOWNGRADING SCHEDULE

16 DISTRIBUTION STATEMENT (of this Report)

APPROVED FOR PUBLIC RELEASE, DISTRIBUTION UNLIMITED

17 DISTRIBUTION STATEMENT (of the abstract entered in Block 20, if different from Report)

18 SUPPLEMENTARY NOTES

ARPA Order No. 2551

19 KEY WORDS (Continue on reverse side if necessary and identify by block number)

Seismology
Automatic Detectors
Fisher Detector
Power Detector
Korean Seismic Research Station

20 ABSTRACT (Continue on reverse side if necessary and identify by block number)

The Fisher detector and conventional power detector have been implemented on short-period data recorded at the Korean Seismic Research Station. It was found that false alarm rates varied so widely from day to day that no comparison between detectors could be made. However, a comparison between detectors with different integration times but the same false alarm rate revealed that integration time does not affect the probability of detection

DD FORM 1 JAN 73 1473 EDITION OF 1 NOV 65 IS OBSOLETE

20. Continued.

A means to hold the alarm rate constant should be developed to permit comparison and evaluation of these detectors.

ABSTRACT

The Fisher detector and conventional power detector have been implemented on short-period data recorded at the Korean Seismic Research Station. It was found that false alarm rates varied so widely from day to day that no comparison between detectors could be made. However, a comparison between detectors with different integration times but the same false alarm rate revealed that integration time does not affect the probability of detection. A means to hold the alarm rate constant should be developed to permit comparison and evaluation of these detectors.

Neither the Advanced Research Projects Agency nor the Air Force Technical Applications Center will be responsible for information contained herein which has been supplied by other organizations or contractors, and this document is subject to later revision as may be necessary. The views and conclusions presented are those of the authors and should not be interpreted as necessarily representing the official policies, either expressed or implied, of the Advanced Research Projects Agency, the Air Force Technical Applications Center, or the US Government.

TABLE OF CONTENTS

LIST OF FIGURES

LIST OF TABLES

SECTION I
INTRODUCTION

This report presents results of a study of two seismic signal detectors; the Fisher detector and the conventional power detector. These detectors have been described in an earlier report (Lane, 1973), herein called Report 1, where their performance on long-period data was studied. The present report is concerned with their response to short-period data at the Korean Seismic Research Station (KSRS).

A total of 185 events were processed by the detectors and the results used to estimate a probability of detection for magnitudes greater than 3.0. A number of hour-long noise samples were also processed to find false alarm rates. A simple quality-control algorithm was devised to remove spiked and dead channels.

SECTION II
ALGORITHMS, DEFINITIONS, AND DATA

A. ALGORITHMS

Both the Fisher and conventional power detector reported on here have been described from a theoretical and experimental point of view in Report I. Each searches the time-delayed data for signal-like characteristics. In the case of the Fisher detector this characteristic is waveform similarity. If the time-aligned traces are designated by y_i, the Fisher detector output is

$$F = \frac{(M-1)\left\{\overline{\frac{1}{M}\sum_{i=1}^{M} y_i}\right\}^2}{\overline{\frac{1}{M}\sum_{i=1}^{M} (y_i)^2} - \left\{\overline{\frac{1}{M}\sum_{i=1}^{M} y_i}\right\}^2} \qquad \text{II-1}$$

where M is the number of channels and the bar denotes an equally weighted average over some previous time interval, called the integration time. When all the y_i are the same, the denominator of II-1 is zero, because under these conditions the mean square of the y_i is equal to their squared mean. When the y_i are perfectly uncorrelated, the detector output, as normalized,

is one. A real signal will always be accompanied by noise, and for the case of propagating undistorted plane wave signals with noise correlated neither with itself nor the signal, the detector output can be shown to be equal to

$$F = \frac{S^2 + N^2}{N^2} \qquad \text{II-2}$$

where S^2 is the signal power and N^2 is the noise power.

Real signals are generally dissimilar from site to site as well as noisy, and the Fisher detector output is reduced in this case. Expressions for this reduced output are derived in Report 1, where it is shown that the detector saturates at an output level dependent on the kind and degree of distortion.

The conventional power detector forms the ratio of the short-term average beam power to the long-term average beam power. The short-term average is equally weighted over its time gate, while the long-term average is exponentially weighted into the past. The detector output is then

$$P = \frac{\left\{ \frac{1}{M} \sum_{i=1}^{M} y_i \right\}^2}{\sigma_o^2} \qquad \text{II-3}$$

where σ_o^2 is the long-term average and the other terms are defined as above. For undistorted plane wave propagation the output is again equal to equation II-2 and the limiting values for zero signal and zero noise are the same. The conventional detector is less affected by deviation from plane wave behavior

than the Fisher detector, however, since it merely requires that the power increase on all channels, rather than that the channels be similar. It saturates at a higher level for the same degree and kind of distortion.

Both the Fisher and conventional power detectors involve a number of characteristic times. These include the upper and lower cut-off periods of the prefilter, the long-term averaging time for the conventional detector, and the integration times for the detector outputs. To pick tentative values for these times, each time was scaled from its value in the long-period detector by the ratio of the periods of peak motion in the short and long-period data. This ratio was about .025, so starting values for the integration times were chosen to be 0.8 to 6.4 seconds, and the data were band-pass filtered between 0.3 and 2.0 seconds. The time constant for the long-term average was reduced to 6 seconds.

A simple quality check was devised to remove faulty data. In this algorithm the power for each channel was averaged over about 24 seconds, and the median channel power found. Channels with powers differing from this value by more than a factor of 3 in either direction were discarded. This procedure was as successful at detecting spiked or dead channels as inspection of the time traces in all cases where the traces were examined.

B. DEFINITIONS

The detectors studied here involve only one output, as defined in equations II-1 and II-3. When this output rises above some pre-determined value, called the detection threshold, it is claimed that a seismic signal is present. A log of such claimed detections is kept, and an analyst may later confirm or reject each one, although this was not done in the present report.

The detector output may rise above the threshold for some reason other than the presence of a real signal. This is called a false alarm, and an assessment of the rate at which these alarms occur is an important part of the detector evaluation.

Conversely, the detector may not respond sufficiently to a real signal, due to distortion or masking noise. The probability of detection of a class of events is the fraction of those events for which the detector output rose above some threshold. This is also an important detector characteristic and, like the false alarm rate, is dependent on threshold setting.

C. DATA

The Korean Seismic Research Station (KSRS) is located in Korea, at 37° 27' North latitude and 127° 54' East longitude. It consists of a 19 element hexagonal array of short-period instruments arranged in two concentric rings about a center element.

Inter-element spacing is about 2.5 kilometers, roughly half that at the NORSAR short-period array. KSRS also has an array of seven long-period instruments; however, these instruments were not used in this study. The short-period data, for the vertical component only, are recorded on magnetic tape at the rate of 20 points per second.

Data are available on library tapes of 8 hour duration, and one such tape was present for every alternate day starting 29 April 1973, and ending 26 July 1973. This represents 360 hours of data over a three-month period. During the time covered by the tapes 185 seismic events of magnitude equal to or greater than 3.0 and of epicentral distance less

than 80 degrees but greater than 20 degrees from KSRS were reported in the NORSAR and LASA bulletins. These events form the data base for this report. A histogram of their distribution with magnitude is shown in Figure II-1, and their distribution by region is shown in Table II-1.

Events of epicentral distance less than 20 degrees were excluded from this study. At this distance, waveform similarity from site to site is poor, and time delays are calculated less accurately from plane wave models than for more distant events. Thus the Fisher detector, and to a somewhat lesser extent the conventional power detector, would not be expected to respond to these events.

These events are not within the area of interest since they are largely in the Japanese Islands. If they were included in the data base, they would significantly bias the detection probability downward since there are about two thirds as many events reported within 20 degrees as beyond. Therefore, these events have been treated as noise. They have not been included in the data base as events, nor excluded from the "signal-free" noise samples. Their presence in the noise samples may increase the false alarm rate, but will do so just as in an operational detector.

Examination of the NORSAR, and LASA bulletins revealed that no events were reported during the following time intervals:

Day	Hours
131	03:00:00 to 04:00:00
141	13:30:00 to 14:30:00
161	13:30:00 to 14:30:00
183	09:00:00 to 10:00:00

These samples were used to calculate noise statistics.

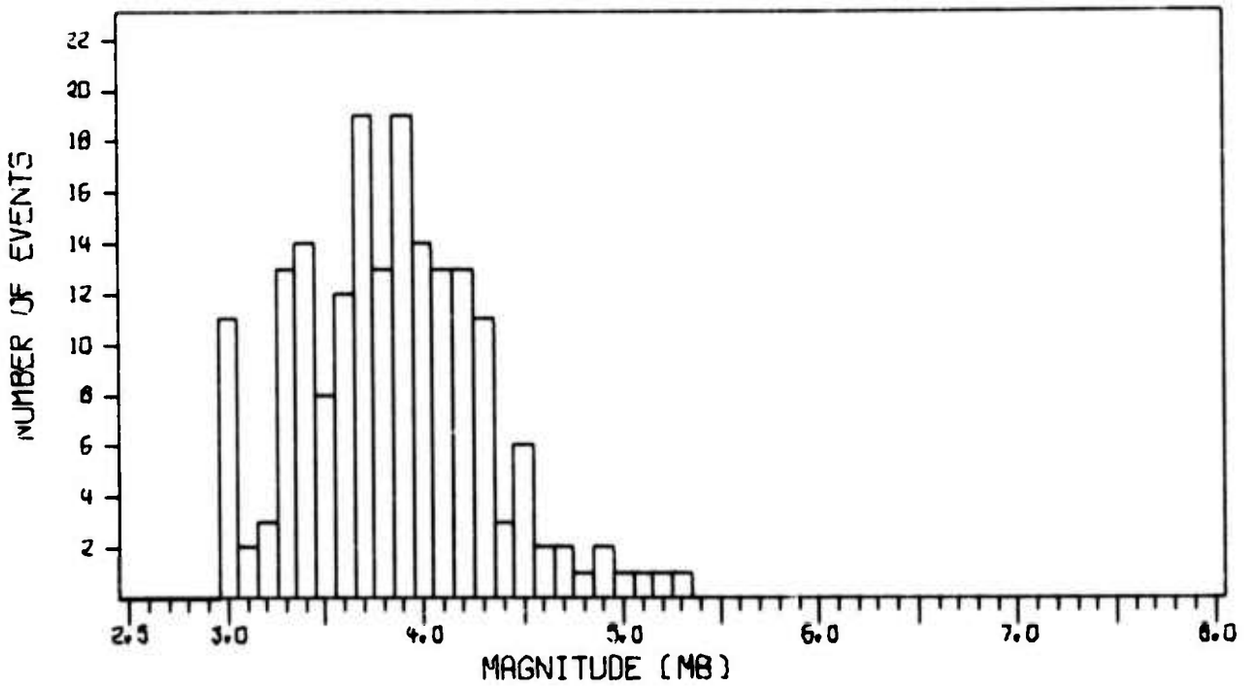

FIGURE II-1

HISTOGRAM OF NUMBER OF EVENTS BY MAGNITUDE

TABLE II-1

DISTRIBUTION OF PROCESSED EVENTS BY REGION

Region	Number Of Events
Kurile Islands, Kamchatka, Alaska	69
Pacific Islands	44
Mediterranian Basin	20
China and Eastern Russia	21
Western Russia	21
Miscellaneous	10
Total	185

The quality of the data was low. Dead channels and spikes were common, but these data were removed to a large extent by the quality check. From as few as 7 to as many as all 19 channels were available at various times.

Delay times found by visually aligning traces agreed well with those predicted by a plane wave model. However, amplitude distortion, probably due to the recording system, was sometimes noted and has been observed by others as well (Der, 1974).

SECTION III

FALSE ALARM RATE

To find the response of the detectors to pure noise, the hour-long noise samples mentioned in Section II were processed with each detector. The detectors used integration times of 0.8, 1.6, 3.2 and 6.4 seconds and formed 16 km/sec beams in twelve directions, evenly spaced at 30 degree intervals. For each azimuth and integration time the output of each detector was quantized at 0.4 dB intervals and displayed every 0.8 seconds in the same form as used for the long-period data in Report 1.

In order to exclude multiple detections from the same event and to reduce the false alarms from imperfectly corrected spikes, a "dead time" of 24 seconds followed the time at which the detector exceeded each quantization level. During this time no more detections at that level were allowed.

The variation in false alarm rate from one azimuth to another was small, so data from all azimuths at a given level were averaged together to produce the false alarm rates shown in Figure III-1. Here the number of detections per hour is plotted versus the threshold value at which those detections occurred. Data for each of the five noise samples studied are shown for the Fisher and conventional detectors having a 0.8 second integration time. Since the 24 second dead time allowed a maximum of 150 detections in one hour, the curves approach this value at the lowest threshold levels.

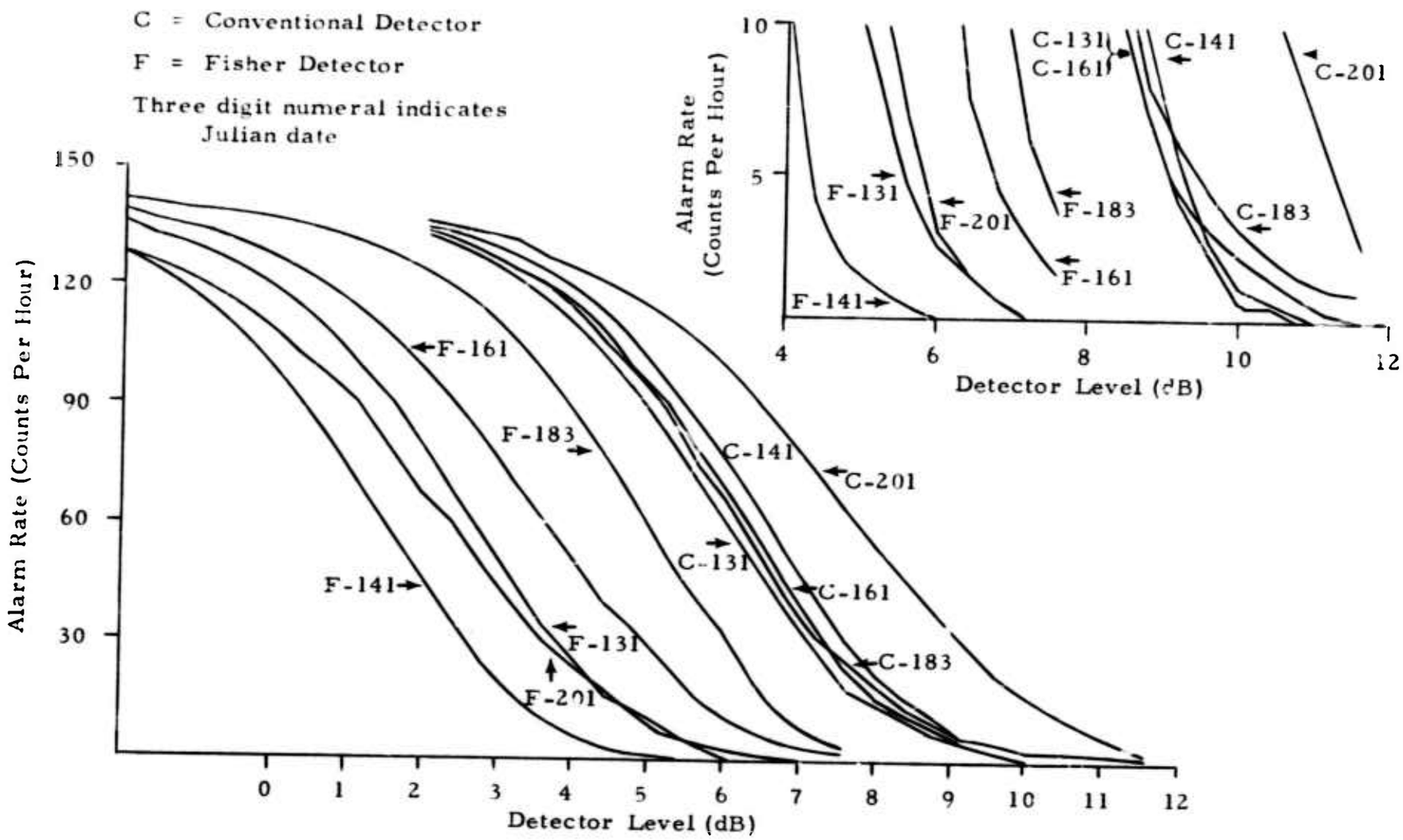

FIGURE III-1

FALSE ALARM RATES PER HOUR FOR FISHER AND CONVENTIONAL DETECTORS AT 0.8 SECOND INTEGRATION TIME

Two broad conclusions may be drawn from these curves. First, the conventional detector consistently shows a higher alarm rate than does the Fisher detector at the same threshold. Second, the variation in false alarm rate from day to day is greater for the Fisher detector than for the conventional detector. Except for day 201, the conventional detector is substantially the same from one day to another. The Fisher detector, however, can vary in false alarm rate by at least a factor of 20 between different days.

The difference in alarm rate between the detectors is not significant without a knowledge of the detection probability, and cannot be used to conclude that one detector is superior to the other. The variation in the Fisher detector's false alarm rate suggests that if the Fisher detector was superior on some days it might not be on others, depending on the nature of the noise.

The root-mean-squared amplitude, averaged over all operating channels and over each hour of noise data, was as shown in Table III-1. Comparison of this table with Figure III-1 shows that there is a general trend for days with high rms noise levels to have low Fisher detector false alarm rates; the results on day 201 are the only exception to this trend. The large difference in behavior of the conventional detector on day 201 from its behavior on other days suggests that some different noise mechanism was operating on that day.

In Report 1 it was shown that spikes in the data reduce the Fisher detector output. When numerous small spikes or large amplitude excursions have been present on noisy days, the Fisher detector has been observed to show a lower alarm rate. The conventional detector averages these spikes over all channels and thus is relatively insensitive to them. On day 201, rapid fluctuations in the noise power about its mean may have produced the observed behavior of the conventional detector.

TABLE III-1

ROOT MEAN SQUARE NOISE AMPLITUDES

Day	RMS Amplitude (Digital Counts)
131	4.8
141	7.5
161	4.5
183	3.8
201	8.8

Figure III-2 shows false alarm rates versus level for the Fisher detector on day 161, for a number of integration times. These behaviors are typical in that the spacing between curves is maintained from day to day, although the curves are displaced as shown in Figure III-1.

The variability of the noise reported here means that a detector using a fixed threshold will be less than optimum. For example, if a false alarm rate of 5 per hour was chosen as satisfactory, experience on day 131 would indicate that a Fisher detector threshold level of 5.6 dB should be chosen. Only 30 days later, on day 161, the rate at this threshold would have risen to about 17 per hour, an unacceptable figure. On the other hand, the false alarm rate on day 141 would have been about one alarm every two hours. Such a low false alarm rate is of course desirable, but on this day a lower threshold would have realized an increased probability of event detection while still keeping the false alarm rate within acceptable bounds.

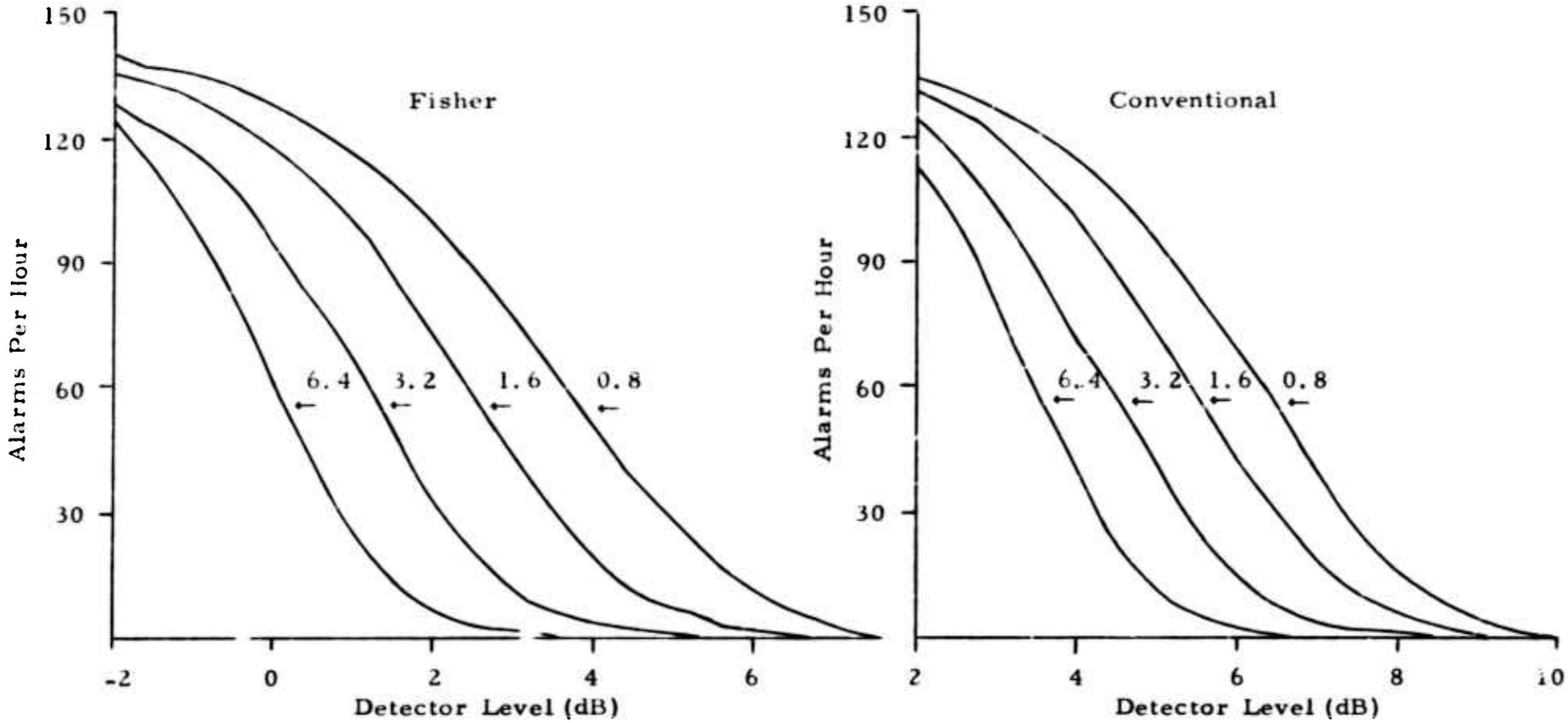

FIGURE III-2

FISHER AND CONVENTIONAL DETECTORS FALSE ALARM RATES
ON DAY 161 AT VARIOUS INTEGRATION TIMES

SECTION IV
DETECTION PROBABILITY

In this section expressions for comparing and evaluating automatic detectors are presented, and some sample results are shown. These curves relate detection probability to magnitude for a given threshold. Since the alarm rates found in section III are so variable, the results shown here are to be regarded as illustrative of the method and to form a standard by which improved versions of these detectors may be judged.

All the events described in Section II-B were processed with both detectors. The largest amplitude of the detector output occurring within 36 seconds of the predicted arrival time on three beams spaced at 15 degrees and centered on the signal azimuth was recorded. The magnitude assigned to the event was that listed by NORSAR or LASA. Then the number of detections and non-detections at each magnitude were found by counting the number of events for which the detector output did or did not exceed an assumed detector level, respectively.

These data were fitted to a model adapted from one developed by Ringdal, (1974). His model assumes that the probability of detecting an event of magnitude M is given by the cumulative Gaussian distribution

$$P(M) = \frac{1}{\sqrt{2\pi\sigma^2}} \int_{-\infty}^{M} e^{-\frac{1}{2}\left(\frac{x-\mu}{\sigma}\right)^2} dx \qquad \text{IV-1}$$

where μ and σ are parameters to be fitted to the observed detection probability. This fitting is done so as to maximize the likelihood function associated with equation IV-1. The function P(M) is called the detection curve.

This theory assumes that the probability of detecting a sufficiently small event is zero. For the automatic detector there is a probability related to the false alarm rate that the detector level will exceed the threshold within the signal arrival time window due to noise. This probability of incorrectly detecting small events was incorporated into the maximum likelihood approach by modifying equation IV-1 to read

$$P(M) = K + (1-K) \frac{1}{\sqrt{2\pi\sigma'^2}} \int_{-\infty}^{M} e^{-\frac{1}{2}\left(\frac{x-\mu'}{\sigma'}\right)^2} dx \qquad \text{IV-2}$$

Here K is the constant detection probability at small magnitude, and is found by the fitting process as are μ' and σ'. As a practical matter, it is impossible to estimate accurately three parameters from the limited data sample available, so the results here should be regarded as illustrations of the method.

An example of a detection curve and the assocated histogram of detections and non-detections are shown in Figure IV-1 for the Fisher detector at 0.8 second integration time and threshold level of 5.2 dB. The small magnitude detection probability is .15, and MB50 and SIGMA are μ' and σ' respectively. Confidence limits for this curve are difficult to calculate when variations in K are allowed, and those shown do not account for this variation. This problem will be overcome in the future by fixing K before maximizing the probability function.

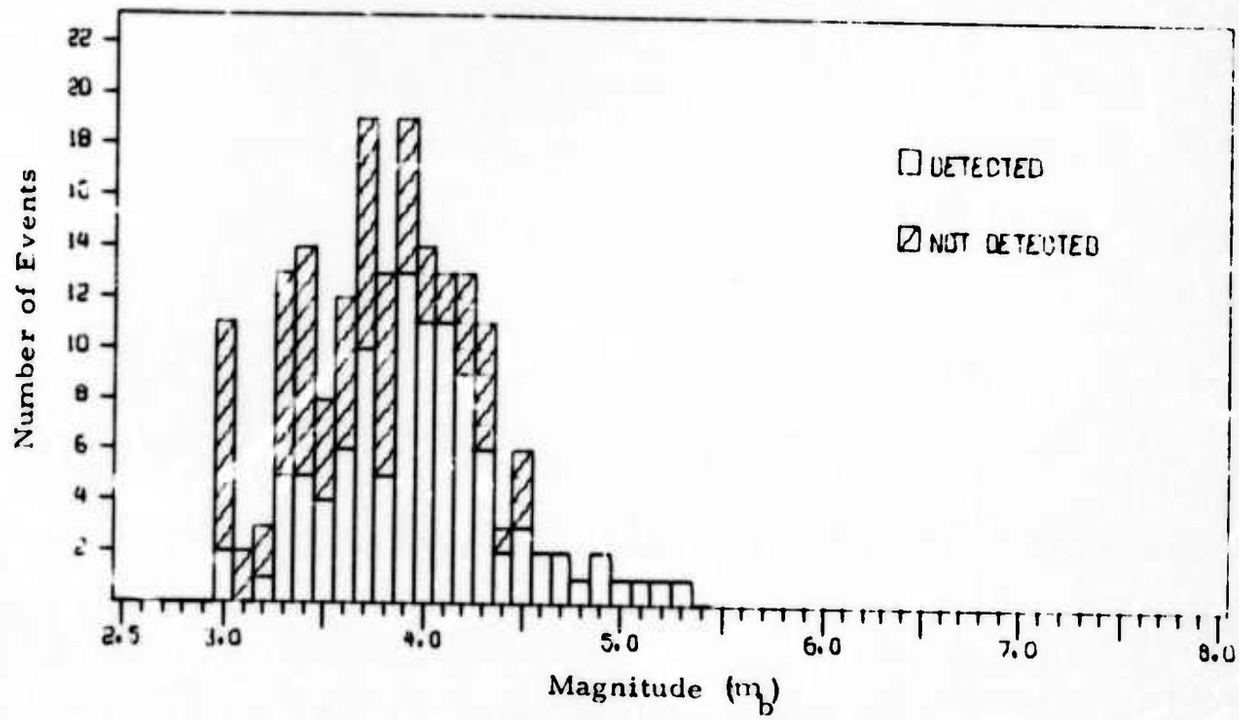

FIGURE IV-1a

DISTRIBUTION OF PROCESSED EVENTS BY m_b

0.8 SECOND FISHER DETECTOR AT LEVEL 5.2 dB

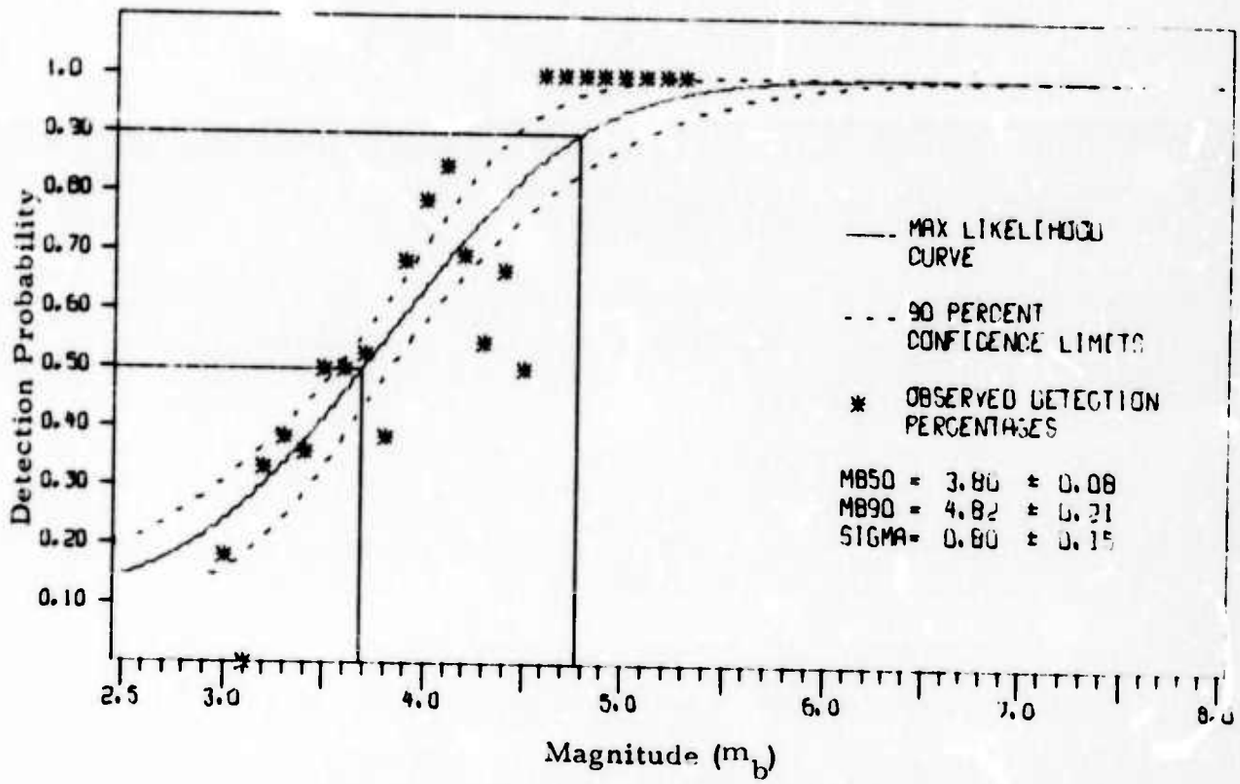

FIGURE IV-1b

MAXIMUM LIKELIHOOD DETECTABILITY CURVE
0.8 SECOND FISHER DETECTOR AT LEVEL 5.2 dB

When the analyst checks the claimed detections on which the curve of Figure IV-1b is based, he will reject those which are due to noise virtually every time. Therefore, this curve lies above the true detection curve given by

$$P(M) = \frac{1}{\sqrt{2\pi\sigma'^2}} \int_{-\infty}^{M} e^{-\frac{1}{2}\left(\frac{x-\mu'}{\sigma'}\right)^2} dx \qquad \text{IV-3}$$

where the parameters are determined from the model equation IV-2. This curve is the probability of confirmed detections as a function of magnitude. It and equation IV-2 are shown in Figure IV-2 for the data of Figure IV-1.

The small magnitude intercept of the observed detection curve is the probability that a detector output equal to or greater than the threshold occurred at least once in three 24 second intervals on three adjacent azimuths, due to noise alone. Let the probability of a false alarm be P_{24} per 24 seconds. Then the probability of no false alarm over all three azimuths for 72 seconds is $(1-P_{24})^n$, where n = 3 if the data are perfectly correlated from azimuth to azimuth and = 9 if they are perfectly uncorrelated. This probability of no alarm for the data of Figure IV-1 is

$$1 - .15 = .85 = (1-P_{24})^n \qquad \text{IV-4}$$

giving a range for P_{24} of 0.05 to 0.02, corresponding to a range of 7.5 to 3 false alarms per hour. Reference to Figure III-1 shows that this rate is reasonable.

The uniformity from day to day in the spacing of the false alarm curves for various integration times displayed in Figure III-2 means that a comparison of detectors at different integration times can be made. For this purpose the detection curve for the Fisher detector using a 6.4 second integration time was calculated assuming a threshold of 1.6 dB.

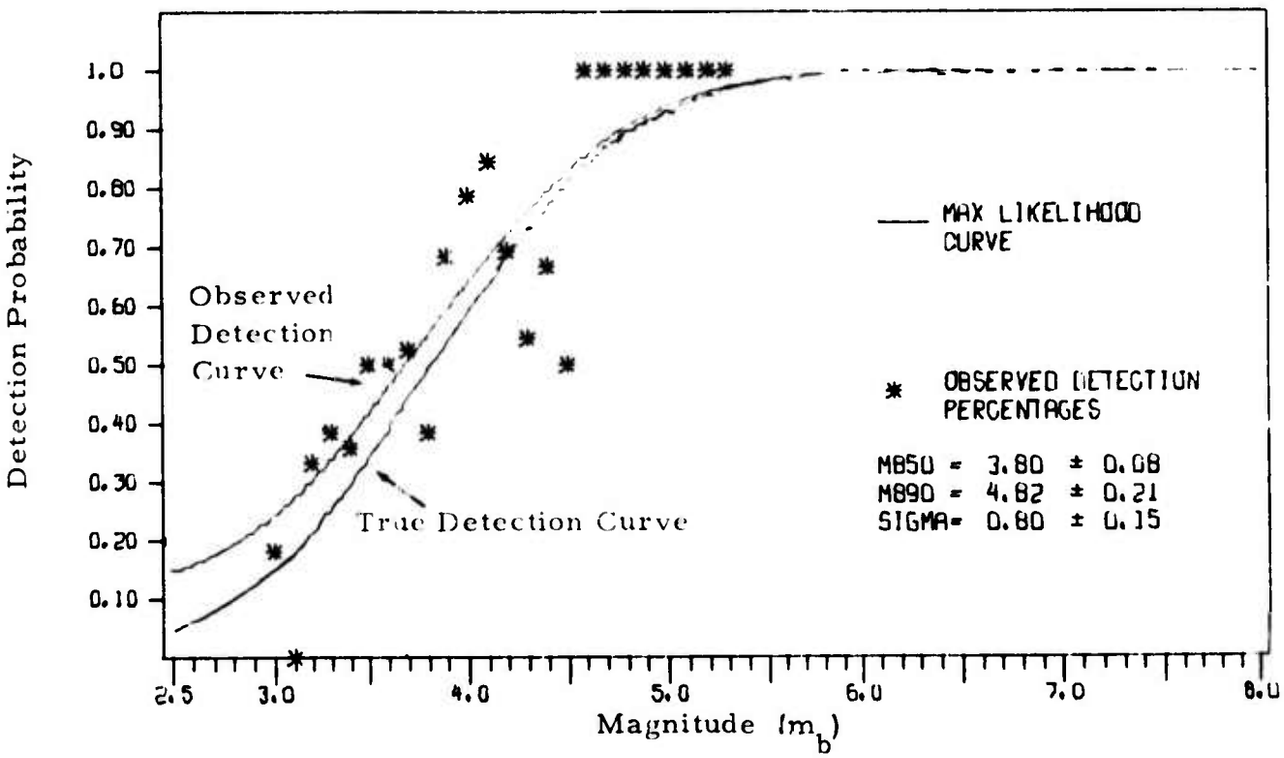

FIGURE IV-2

MAXIMUM LIKELIHOOD DETECTABILITY CURVE
TRUE AND OBSERVED FISHER DETECTOR
AT LEVEL 5.2 dB

This level should give a false alarm rate comparable to that achieved with the Fisher detector using a threshold of 5.2 dB and an integration time of 0.8 seconds, according to the discussion of Figure III-2. The detection histogram and curve are shown in Figure IV-3a and IV-3b.

The curve in Figure IV-3b is indistinguishable from that of Figure IV-1b. The difference in small magnitude detection probability, 0.1 in Figure IV-1b and 0.15 in Figure IV-3b, is no larger than might be expected, given the small number of events in the data sample. Consequently, we can conclude that there is no discernible difference between the Fisher detectors using 6.4 and 0.8 second integration times when the thresholds are adjusted to give a constant false alarm rate. A similar experiment shows that there is likewise no difference between the 0.8 second and 6.4 second conventional detectors, for levels which give comparable false alarm rates.

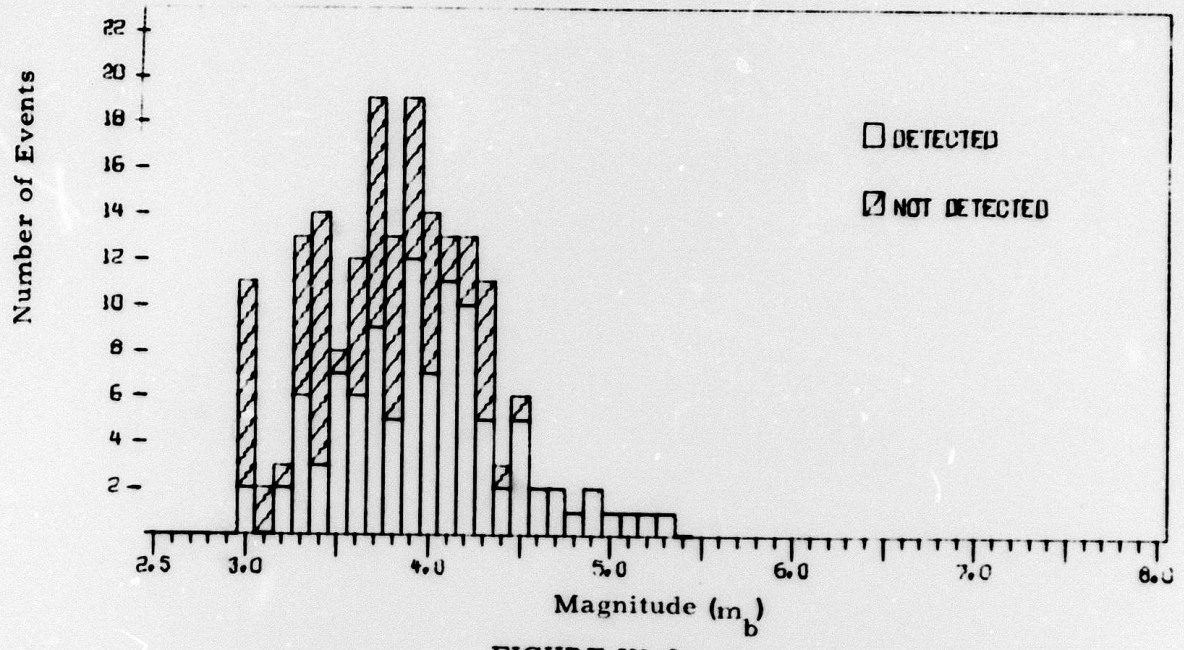

FIGURE IV-3a

DISTRIBUTION OF PROCESSED EVENTS BY m_b
6.4 SECOND FISHER DETECTOR AT LEVEL 1.6 dB

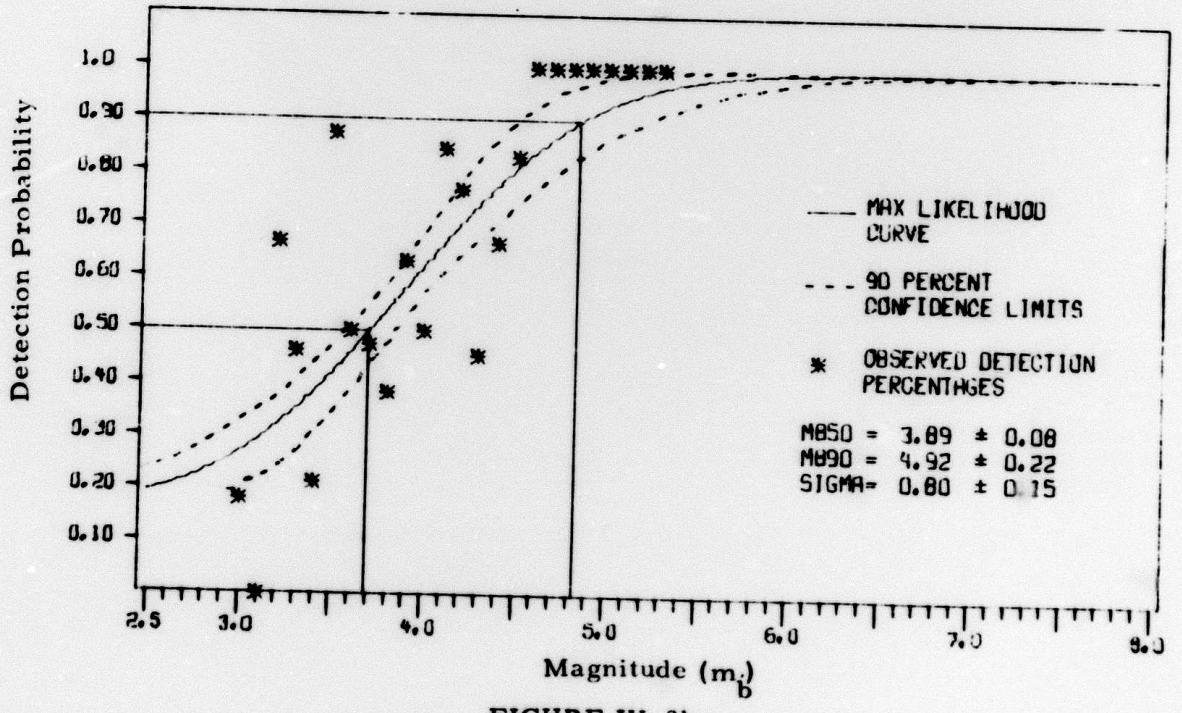

FIGURE IV-3b

MAXIMUM LIKELIHOOD DETECTABILITY CURVE
6.4 SECOND FISHER DETECTOR AT LEVEL 1.6 dB

SECTION V
CONCLUSIONS

Fisher and conventional beam power seismic event detectors similar to those reported on previously have been developed for short-period data and subjected to a preliminary analysis on short-period data from the Korean Seismic Research Station.

It was found that the false alarm rates produced by the Fisher detector when using fixed detector thresholds varied by as much as a factor of 20 from day to day. For the conventional detector, however, variations in the false alarm rate were smaller and occurred less often. The Fisher detector threshold level for a given false alarm rate was consistently lower than that for the conventional detector. Increased noise power generally resulted in lower Fisher detector false alarm rates, but caused little change in the conventional detector alarm rate. Increasing the integration time of the detectors decreased the false alarm rate in a regular manner.

A total of 185 events which occurred in the spring of 1973 were analyzed with both detectors. Detection curves for a few fixed threshold levels and integration times were developed taking into account the possibility of incorrect detections at small magnitudes. These curves suggest that neither the conventional detector nor the Fisher detector is affected by changing the integration time while keeping the false alarm rate constant.

The wide variation in false alarm rates at a fixed detector threshold means that a detector operating with a fixed threshold will not be optimum. It also means that the performance of such Fisher and conventional detectors cannot be compared directly. Optimum detectors, which maintain fixed alarm rates, could be used for this purpose. At a constant alarm rate, whichever detector had the higher probability of detection would unambiguously be the better detector.

SECTION VI
REFERENCES

Der, Zoltan A., 1974, Personal Communication.

Lane, Stephen S., 1973, Preliminary Comparison of Automatic Fisher and Conventional Power Detection Algorithms, Special Report No. 16, Texas Instruments Report Number ALEX(01)-STR-73-16, AFTAC Contract Number F33657-72-C-0725.

Ringdal, Frode, 1974, Estimation of Seismic Detection Thresholds, Technical Report Number ALEX(01)-TR-74-02, AFTAC Contract Number F08606-74-C-0033.